analytical chemistry

pubs.acs.org/ac Article

Bisphenol A Electrochemical Sensor Using Graphene Oxide and β-Cyclodextrin-Functionalized Multi-Walled Carbon Nanotubes

Arif U. Alam and M. Jamal Deen*

Cite This: *Anal. Chem.* 2020, 92, 5532−5539 Read Online

ACCESS | Metrics & More | Article Recommendations | Supporting Information

ABSTRACT: Bisphenol A, an endocrine disrupting compound, is widely used in food and beverage packaging, and it then leaches in food and source water cycles, and thus must be monitored. Here, we report a simple, low-cost and sensitive electrochemical sensor using graphene oxide and β-cyclodextrin functionalized multiwalled carbon nanotubes for the detection of BPA in water. This sensor electrode system combines the high surface area of graphene oxide and carbon nanotubes, and the superior host−guest interaction capability of β-cyclodextrin. A diffusion-controlled oxidation reaction involving equal numbers of protons and electrons facilitated the electrochemical sensing of BPA. The sensor showed a two-step linear response from 0.05 to 5 μM and 5−30 μM with a limit of detection of 6 nM. The sensors also exhibited a reproducible and stable response over one month with negligible interference from common inorganic and organic species, and an excellent recovery with real water samples. The proposed electrochemical sensor can be promising for the development of simple low-cost water quality monitoring system for monitoring of BPA in water.

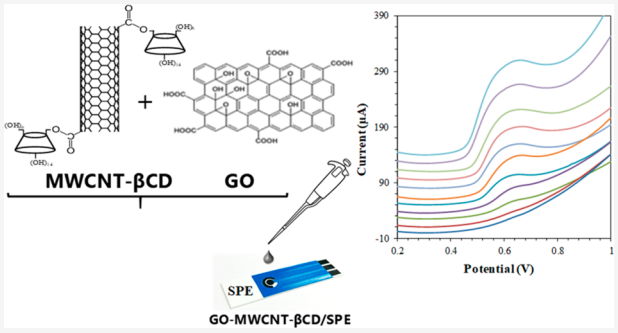

Bisphenol A (BPA), scientifically known as 2,2′-bis(4-hydroxyphenyl)propane), is one of the most highly used chemicals worldwide for synthesizing polycarbonate and epoxy resins, being used for food-storage, packaging, feeding bottles, and beverage cans.[1] The widespread use of BPA has caused its exposures to human and aquatic organisms through leaching into food and water from packaging materials.[2] The presence of phenol groups in the structure of BPA is similar to those in endocrine hormones, specifically estradiol and diethylstilbestrol, causing it to bind to estrogen receptors.[3] Thus, BPA is known as an endocrine disrupting compound (EDC).[4] Low doses of BPA along with other emerging contaminants such as pain-killers and hormones at subnanogram levels can affect human and aquatic health.[5−7] For example, exposure to BPA adversely affects the functions of brain, thyroid, ovary, and reproductive organs, leading to cardiovascular diseases, obesity, carcinogenicity, neurotoxicity, and child developmental problems.[8,9] Therefore, BPA has been declared as a toxic substance in many countries by their regulatory agencies.

The main source of BPA exposure in humans are food, drinks, and water due to its migration from the plastic containers to the food products. The predicted-no-effect-concentrations (PNEC) of BPA in water were declared as 1.5 and 0.175 μg/L by European Union and Canada, respectively.[10] BPA concentrations in few nanomolar range can mimic estradiol hormone and result in changes in some cell functions.[11] Therefore, predicting the exposure and potential health effects of BPA requires its frequent monitoring in drinking water. Conventional analytical techniques such as liquid chromatography, liquid chromatography−mass spectrometry, gas chromatography−mass spectrometry, and enzyme-linked immunosorbent assay are commonly used by regulatory agencies for the determination of BPA.[12] However, these methods are expensive, time-consuming, and require trained personnel to perform tedious extraction processes. Therefore, the development of new methods for the determination of BPA at trace concentrations has become a major research challenge. Recently, electrochemical techniques were shown to be promising for simple, rapid, and accurate determination of BPA due to their simple fabrication, small foot print, high sensitivity, wide linear range, and minimal sample preparation.[13,14]

Electrochemical sensing of BPA requires the use of a working electrode which is modified by different nanomaterials such as carbon nanostructures, metal nanoparticles,[15] polymers,[16] ionic liquid,[17] and/or their combinations.[18−20] Among these, carbon nanomaterials, such as carbon nanotubes (CNTs) and graphene were extensively utilized in electrochemical sensing for environmental and healthcare application.[20−23] For example, CNTs can be functionalized/modified

Received: January 28, 2020
Accepted: March 6, 2020
Published: March 6, 2020

https://dx.doi.org/10.1021/acs.analchem.0c00402
Anal. Chem. 2020, 92, 5532−5539

Scheme 1. Schematic Diagram of the Preparation of GO-MWCNT-βCD/SPE Electrode

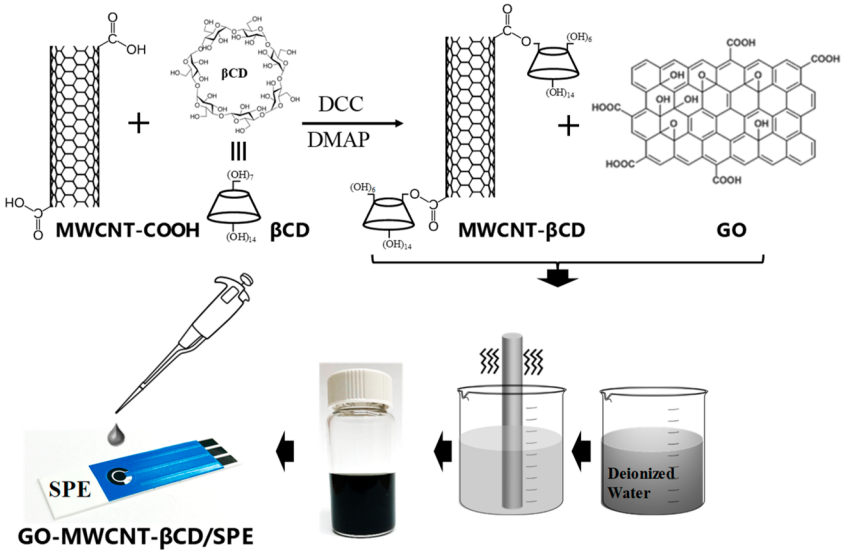

with different chemical groups such as acids/amines,[24] biomolecules such as tyrosinase,[25] aptamers,[26] and engineered recognition sites using molecularly imprinting,[27] to enhance its sensing performance of BPA. However, several disadvantages limit the development of simple and low-cost sensors for BPA using CNTs. For example, the covalent functionalization of CNTs is usually complex and requires multiple chemical reaction steps. In addition, electrochemical functionalization of CNTs with polymers mostly requires the use of monomers and reagents that are sensitive to oxygen and moisture. Also, getting a uniform thin layer of CNTs through drop-casting of aqueous CNTs suspension requires dispersion with a surfactant.[28] Moreover, CNTs cannot achieve high sensitivity to BPA alone, thus necessitating conjugation with other molecules and nanostructures that can improve the sensing performance through enhanced electrochemically active surface area, synergistic electrocatalytic effects, and high selectivity or affinity to the BPA molecule.

To address these challenges, the large effective surface area and strong electrochemical oxidation capability of graphene oxide (GO) and multiwalled CNTs (MWCNTs) in combination with the host−guest interaction capabilities of β-cyclodextrin (βCD) can be used.[29−31] The βCD is a seven-membered cyclic oligosaccharides, commonly used in food, pharmaceutical, drug delivery, and chemical industries.[32,33] βCD is also known to encapsulate organic micropollutants including BPA in the form of well-defined host−guest complexes.[34,35] Recently, we studied noncovalent/covalent functionalization of MWCNTs with βCD that showed enhanced electrochemical sensing performance toward the detection of acetaminophen and estrogen.[6,7] However, there are limited reports on βCD modified electrodes for the detection of BPA.[36,37] Also, the sensing capability of one-step, covalently functionalized MWCNT-βCD together with the synergistic electrochemical sensing effects of GO for the detection of BPA is yet to be investigated. The conjugation of GO with the MWCNT-βCD molecules facilitated the development of a simple, low cost and highly sensitive electrode for BPA sensing.

In this paper, we develop a simple, easy-to-use and low-cost electrochemical BPA sensor based on a composite of GO and covalently functionalized MWCNT-βCD which were then used to modify screen-printed carbon electrode. The composite was first prepared through the one-step Steglich esterification of MWCNT-COOH with βCD to make MWCNT-βCD followed by the mixing with GO, which were subsequently dispersed in water. The resulting electrode GO-MWCNT-βCD/SPE was prepared by drop casting the GO-MWCNT-βCD suspension into SPE. The modified GO-MWCNT-βCD/SPE electrode was electrochemically characterized by cyclic voltammetry, and then used to detect BPA through linear sweep voltammetry. To the best of our knowledge, there is no report on one-step modification of MWCNT−βCD and their conjugation with GO to detect BPA. The modified electrode combines the electrocatalytic properties of MWCNTs, the selective host−guest inclusion capability of βCD, and the synergistic electrochemical sensing effect of GO for simple, low-cost, and highly sensitive determination of BPA. The sensitivity, linear range, limits of detection, interference, and measurements in real water samples were also demonstrated. The proposed electrochemical sensor provides opportunities for developing a smart, low-cost, and easy-to-use system for water quality monitoring.

EXPERIMENTAL SECTION

Reagents and Materials. COOH-functionalized MWCNT (MWCNT-COOH, > 95%, OD: 5−15 nm, length: ∼50 μm, electrical conductivity: >100 S/cm) were purchased from U.S. Research Nanomaterials Inc. Bisphenol A (BPA), β-cyclodextrin, GO suspension (794341, 1 mg/mL dispersion in water) and phosphate buffer solution (PBS) tablets (P4417) were purchased from Sigma-Aldrich. All chemicals were of analytical standards and were used without further purification. The aqueous solutions were prepared with deionized (DI) water (≥18 MΩ cm). One PBS tablet was dissolved into 200 mL of DI water to make 0.01 M phosphate buffer solutions (PBS) at pH 7.4. The 0.01 M acetate buffer solutions at pH 4 and 5 were prepared by dissolving appropriate amounts of acetic acid (CH_3COOH) and sodium acetate (CH_3COONa) into DI water. Similarly, pH 6, 7, and 8 buffer solutions were prepared by dissolving appropriate amounts of Na_2HPO_4, and

https://dx.doi.org/10.1021/acs.analchem.0c00402
Anal. Chem. 2020, 92, 5532−5539

NaH_2PO_4; and pH 9 and 10 buffer solutions were prepared by dissolving appropriate amounts of boric acid (H_3BO_3) and sodium tetraborate ($Na_2B_4O_7$) into DI water.

Apparatus. All measurements were carried out with conventional three-electrode potentiostat cell. A PalmSens EmStat 3 potentiostat (from PalmSens.com) was connected to the three-electrode cell controlled by a laptop computer (Intel Core i5, 2400 MHz) and PSTrace 5.3 software. The three-electrode cell contained a platinum auxiliary electrode, an Ag/AgCl reference electrode and SPE working electrode. The working electrode had an exposed area of 0.070 cm^2, which was modified with GO-MWCNT-βCD composite material. All the electrodes were purchased from CH Instruments. Cyclic voltammetry (CV) measurements of SPE electrodes modified with GO, MWCNT-βCD, and GO-MWCNT-βCD were done in 5 mM $K_3[Fe(CN)_6]$ with 0.1 M KCl solution to calculate the electrochemically active surface area. All measurements were performed at 25 ± 2 °C.

Preparation of the GO-MWCNT-βCD Modified Electrode. The covalent modification of MWCNTs with βCD was done by a one-step Steglich esterification reaction.[7] In brief, MWCNT-COOH was dispersed in anhydrous *N*,*N*-dimethylformamide by ultrasonication in an inert (Ar gas) environment. The 4-(dimethylamino)pyridine, βCD and dicyclohexylcarbodiimide were added to the suspension at 0 °C. The resulting suspension was then vigorously stirred for five hours at 20 °C. The precipitated MWCNT-βCD was filtered through a nylon membrane. The excess DCC, DMAP, and unreacted βCD was removed by repeated washing with DMF and acetone. An ultrasonic preprocessor was used to make a uniform suspension of the covalently modified MWCNT-βCD by dispersing 40 mg of the MWCNT-βCD powder into 20 mL of DIW. The 2 mg/mL MWCNT-βCD suspension was then added with GO suspension (1 mg/mL) in 1:1 volume ratio and ultrasonicated for 2 h to get a uniform GO-MWCNT-βCD suspension. Finally, an aliquot of 10 μL GO-MWCNT-βCD suspension was drop-casted on SPEs and dried in air for 4 h to get GO-MWCNT-βCD/SPE electrodes. Scheme 1 shows a simple illustration of the electrode fabrication processes. For comparison, SPEs were also modified by drop casting 10 μL of GO, MWCNT, and MWCNT-βCD in SPE and dried in air for 4 h to get GO/SPE, MWCNT/SPE, and MWCNT-βCD/SPE electrodes, respectively.

RESULTS AND DISCUSSIONS

Electrochemical Sensing Performance of GO-MWCNT-βCD/SPE Electrode. The sensing performance of a modified electrode depends on its electrochemical oxidation capability with the target analyte (i.e., BPA). To enhance the sensing performance, the high surface area of MWCNTs[38] and the analyte-capturing ability of βCD[39] can be utilized. Figure 1 shows the comparison of linear sweep voltammetry (LSV) results with MWCNT, MWCNT-βCD, GO, and GO-MWCNT-βCD modified SPE in the presence of 5 μM BPA in PBS at pH 7.4 with a scan rate of 50 mV/s. The LSV method is the similar to CV except that the potential scan is not reversed at the end of the first scan. The MWCNT-βCD/SPE electrode (gold dashed curve) showed an oxidation peak current of 24.5 μA at a peak potential (E_{pa}) of 650 mV as compared to the oxidation peak current (13 μA) of MWCNT/SPE (red dotted curve) at E_{pa} of 605 mV. On the other hand, the GO/SPE electrode (blue dashed curve) showed an oxidation peak current of 20.7 μA at E_{pa} of 615 mV. However,

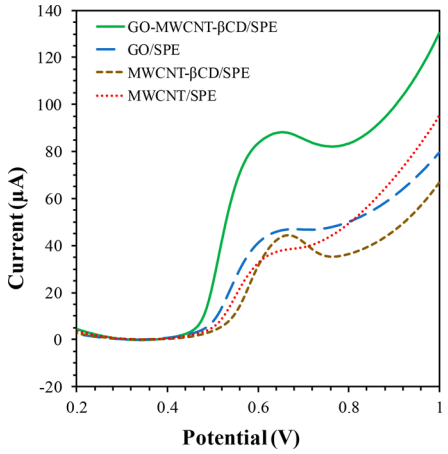

Figure 1. Linear sweep voltammetry (LSV) of MWCNT/SPE (red dotted curve), MWCNT-βCD/SPE (gold dashed curve), GO/SPE (blue dashed curve), and GO-MWCNT-βCD/SPE (solid green curve) recorded in the presence of 5 μM BPA in 0.01 M PBS pH 7.4 at a scan rate of 50 mV/s and accumulation time of 30 min.

the GO-MWCNT-βCD/SPE electrode (green solid curve) showed the highest oxidation peak current of 49.4 μA at E_{pa} of 595 mV. Therefore, it is observed that the BPA oxidation peak current of GO-MWCNT-βCD/SPE was improved by 3.8 times compared to that of MWCNT/SPE, whereas for MWCNT-βCD/SPE and GO/SPE, it was improved by approximately 1.9 and 1.6 times, respectively. The substantial increase in the oxidation peak current of the GO-MWCNT-βCD/SPE electrode may be attributed to their high electrochemically active surface area, excellent oxidation capability, and improved host−guest interaction of the electrode surface with BPA.[7,40] The intensities and positions of these peaks indicates that the GO-MWCNT-βCD/SPE electrode favors an irreversible electrochemical oxidation reaction.

The inherent materials properties of GO and MWCNTs, such as high conductivity and high electron transfer capability, offer an enhanced electrocatalytic activity toward the oxidation of BPA.[41] In fact, the high surface-to-volume ratio of GO and MWCNT provides high number of active electrode surface sites for the oxidation of BPA.[42] Functionalization of MWCNT with βCD enables a synergistic effect by creating a closer contact of BPA molecule due to their porous inner core.[37] The improved oxidation peak current in the presence of βCD and GO can be due to three main factors. First, pure MWCNT provides a single-layer adsorption of BPA. In contrast, the porous βCD on MWCNTs with GO provides a multilayer surface structure to adsorb more BPA, resulting in higher detection sensitivity. Second, covalent functionalization of βCD on MWCNT enhances BPA oxidation through formation of host−guest complexes between βCD and BPA.[7,43] Third, the presence of GO provided even higher surface area and enhanced electrical conductivity and electron transfer between MWCNT-βCD composite matrix. Therefore, the combined effect of βCD on MWCNT and GO provided an increased sensing surface for enhanced detection of BPA.

The role of surface area on the electrochemical behaviors of the electrodes was investigated by analyzing their redox behavior in a standard solution of $K_3[Fe(CN)_6]$ redox probe. Figure 2(a) shows the CV of bare SPE, MWCNT-βCD/SPE, GO/SPE, and GO-MWCNT-βCD/SPE electrodes in an aqueous solution of 5.0 mM $K_3[Fe(CN_6)]$ containing 0.1 M

https://dx.doi.org/10.1021/acs.analchem.0c00402
Anal. Chem. 2020, 92, 5532−5539

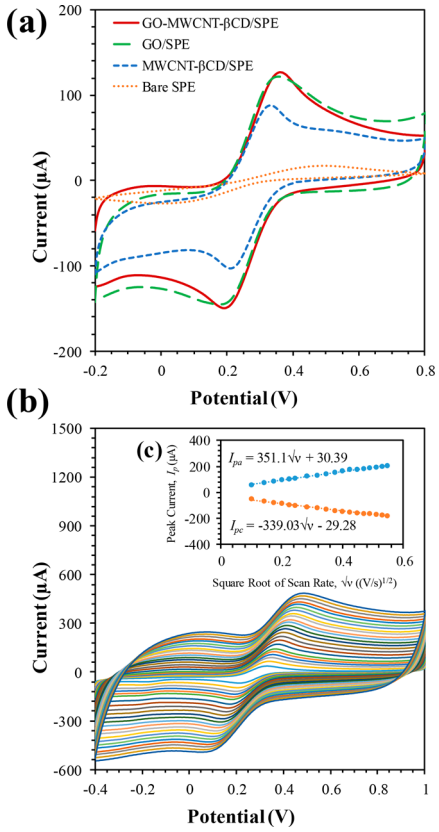

Figure 2. Cyclic voltammetry (CV) curves of different electrodes: bare SPE, MWCNT-βCD/SPE, GO/SPE, and GO-MWCNT-βCD/SPE in an aqueous solution of 5.0 mM $K_3[Fe(CN_6)]$ containing 0.1 M KCl at a scan rate of 50 mV/s. (b) CV curves of GO-MWCNT-βCD/SPE at different scan rate (10, 20, 30, 40, 50, 60, 70, 80, 90, 100, 120, 140, 160, 180, 200, 220, 240, 260, 280, and 300 mV/s) with the same solution. (c) Relationship between peak current vs square root of scan rate derived from the CV curves of Figure 2(b).

KCl at a scan rate of 50 mV/s. The bare SPE electrode showed a pair of redox peaks with peak-to-peak separation (ΔE_p) of 395 mV. For the MWCNT-βCD/SPE, GO-SPE, and GO-MWCNT-βCD/SPE, an increase in the peak current (I_p) and a decrease in the ΔE_p were observed, indicating faster electron transfer. The GO-MWCNT-βCD/SPE electrode showed the highest redox peak currents which is attributed to the excellent electrical conductivity and the larger surface area of the combination of GO, and MWCNT-βCD. For a reversible CV using $K_3[Fe(CN_6)]$, the effective surface area of the modified electrodes can be calculated by using the Randles−Sevcik equation:[44]

$$I_p = 2.69 \times 10^5 A D^{1/2} n^{3/2} \nu^{1/2} C \quad (1)$$

where A is the effective surface area, C is the bulk concentration of $K_3[Fe(CN_6)]$, n is the number of electrons transferred (n = 1), D is the diffusion coefficient of $K_3[Fe(CN_6)]$ (6.67×10^{-6} cm^2 s^{-1}), and ν is the scan rates. Figure 2(b) shows CVs of the GO-MWCNT-βCD/SPE electrodes at a different scan-rate. The square root of scan-rate vs peak current shows a linear relationship as shown in the inset of Figure 2(b). The slope of the I_p-$\nu^{1/2}$ curve (Figure 2(c)) is used in eq 1 to calculate the effective surface area. The effective surface area of GO-MWCNT-βCD/GCE was calculated to be 0.101 cm^2. The area of the bare SPE electrode was 0.070 cm^2, which was amplified by the GO-MWCNT-βCD modification. The high effective surface area can enhance the electrochemical sensing performance of the GO-MWCNT-βCD/SPE electrode for the detection of BPA.

Performance Optimization of GO-MWCNT-βCD/SPE Electrode. Effect of Accumulation Potential and Time. The optimization of the accumulation properties of BPA on the surface of the electrode is essential to determine the optimum experimental condition to achieve highest sensitivity.[45] The accumulation of BPA on the electrode can be achieved through applying a potential (also known as "accumulation potential") for a certain period of time (also known as "accumulation time") with or without magnetic stirring before doing the voltammetry measurements. Applying accumulation potentials (from −0.3 to +0.3) for the GO-MWCNT-βCD/SPE electrode did not improve the oxidation peak current. This could be due to nonpolar behavior of BPA. Therefore, we did not use any accumulation potential for the voltammetric measurements of BPA. However, magnetic stirring of the BPA containing water with the sensing electrode immersed showed significant improvement in the BPA sensitivity. A constant magnetic stirring of 100 rpm was used in all the measurements. The increased sensitivity due to magnetic stirring can be attributed to convection of BPA molecules, which helps to adsorb them on the porous GO-MWCNT-βCD matrix.[7,40] Increasing accumulation time also improved the oxidation peak current of BPA, as shown in Figure 3(a). The BPA oxidation peak current reached to a

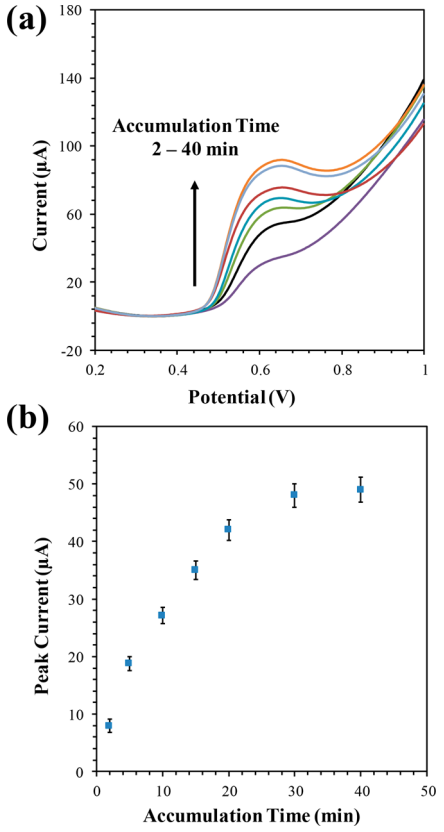

Figure 3. (a) Linear sweep voltammetry (LSV) of GO-MWCNT-βCD/SPE in 5 μM BPA at different accumulation time with scan rate of 50 mV/s. (b) Peak current of the corresponding LSV curves at different accumulation times. Supporting electrolyte: 0.01 M PBS, pH 7.4. Average values were calculated with three determinations.

https://dx.doi.org/10.1021/acs.analchem.0c00402
Anal. Chem. 2020, 92, 5532−5539

stable maximum value with the accumulation time of 30 min, after which it was saturated (Figure 3(b)). Therefore, magnetic stirring of 100 rpm with an accumulation time of 30 min was used in all the BPA sensing measurements.

Effect of Scan Rate. The charge transfer property of a sensing electrode provides important information about electrochemical sensing mechanism. The electron transfer number of the sensing electrodes for the oxidation of BPA is also an important performance indicator. These can be understood by analyzing scan rate (ν) dependent oxidation peak currents and peak potentials for the GO-MWCNT-βCD/SPE in the presence of BPA. Figures 4(a) shows the

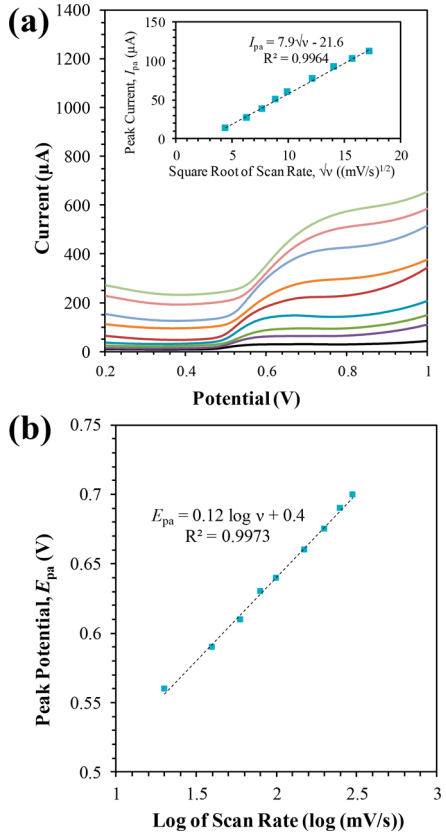

Figure 4. (a) Linear sweep voltammetry (LSV) curves of GO-MWCNT-βCD/SPE in 0.01 M PBS (pH 7.4) with 5 μM BPA at different scan rates (20, 40, 60, 80, 100, 150, 200, 250, 300 mV/s). The inset shows the relationship between the redox peak currents of 5 μM BPA and the scan rates. (b) The dependence of the redox peak potentials of 5 μM BPA on log of scan rate. All the experiments were done with an accumulation time of 30 min and under 100 rpm magnetic stirring before measurements.

relationships between peak potential (E_p) and scan rate (ν) using LSV technique. In the scan rate range of 20 to 300 mV/s, a linear relationship exists between I_{pa} and $\nu^{1/2}$:

$$I_{pa} = 7.9\nu^{1/2} - 21.6(R^2 = 0.9964) \quad (2)$$

The linear relationship between I_{pa} and $\nu^{1/2}$ indicates a diffusion controlled electrode process. Also, a totally irreversible electrochemical oxidation process of BPA with the GO-MWCNT-βCD/SPE gives the following equations relating to E_{pa}:[46]

$$E_{pa} = E_0' + m\left[0.78 + \ln\left(\frac{D^{1/2}}{k_s}\right) - 0.5\ln m\right] + 0.5 \times 2.303 \times \left(\frac{RT}{\alpha n_\alpha F}\right)\log \nu \quad (3)$$

$$E_{pa} - E_{p/2} = \frac{1.857RT}{(\alpha n_\alpha F)} = \left(\frac{47.7}{\alpha n_\alpha}\right)mV(\text{at}25°\text{C}) \quad (4)$$

where E_0' is the standard electrode potential, k_s is the standard heterogeneous rate constant, D is the diffusion coefficient of BPA, α is the transfer coefficient of the oxidation of BPA, $E_{p/2}$ is the potential where $i = I_{p/2}$ in the LSV, and other symbols in eqs 3 and 4 have their usual meanings. According to Figure 4(b), E_{pa} can be expressed with the following equation:

$$E_{pa} = 0.12\log \nu + 0.4(R^2 = 0.9903) \quad (5)$$

From eqs 3 and 5, we find

$$0.5 \times 2.303 \times \left(\frac{RT}{\alpha n_\alpha F}\right) = 0.12 \quad (6)$$

From eq 6, the value of αn_α was calculated to be 0.86. In contrast, the average value of $(E_{pa} - E_{p/2})$ is 60 mV for the scan rate ranging from 20 to 300 mV/s. As a result, the value of αn_α was calculated to be 0.80 from eq 4. The two values of αn_α are almost equal with an average of 0.83. The value of α is assumed to be 0.5 in a totally irreversible electrode process. Therefore, the electron transfer number (n_α) was calculated as 1.7, which is close to 2. This indicates the oxidation process of BPA involved two electrons. In general, higher scan rate provides larger I_{pa}. However, the background current also increases at higher scan rates with increased distortion in the shape of the peak. If the scan rate is too low, the intensity of the oxidation peak will also decrease as the diffusion layer grows much farther from the electrode, resulting in smaller oxidation current toward the electrode.[44] Therefore, an optimum scan rate of 50 mV/s was chosen for the electrochemical sensing of BPA.

Effect of pH. The pH of the solution used is an important parameter as it influences the oxidation potential and peak current when detecting BPA due to shifts of the redox peak potential toward more positive and negative directions with lower and higher pH, respectively.[47] The effect of pH on the oxidation of BPA was studied with the GO-MWCNT-βCD/SPE electrode, as shown in Figure 5. The highest oxidation peak current (I_{pa}) was observed at pH 7, and slowly decreases for lower pH values. However, the peak current was significantly reduced in the pH range 8−10. The decrease in the peak current for higher pH values may be attributed to the electrostatic repulsion of anionic BPA with negative charges on the sensor surface.[48] Hence, pH 7 was chosen as the standard pH for the detection of BPA. On the other hand, the oxidation (E_{pa}) peak potential of BPA shifted negatively with the increase of pH. The linear regression equation for the pH dependent shift of E_{pa} is given as

$$E_{pa} = -0.0655\text{pH} + 1.11(R^2 = 0.9962) \quad (7)$$

The slope of eq 7 can be used to determine the ratio of proton and electron involved in the oxidation reaction using the following relationship:[49]

https://dx.doi.org/10.1021/acs.analchem.0c00402
Anal. Chem. 2020, 92, 5532−5539

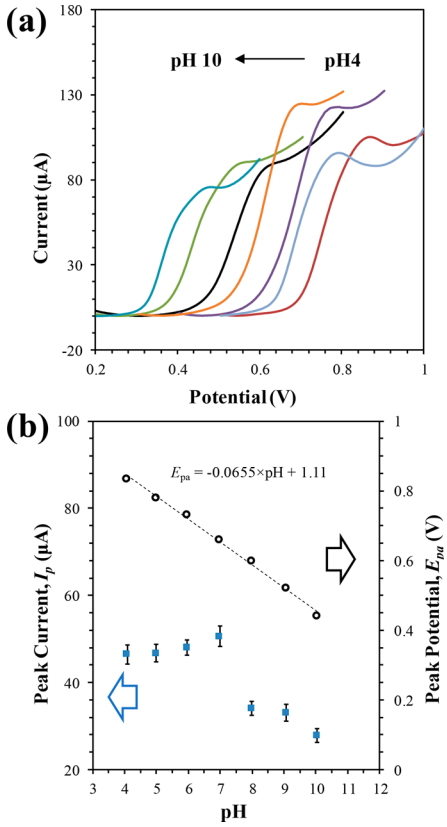

Figure 5. (a) Linear sweep voltammetry (LSV) curves of GO-MWCNT-βCD/SPE in 0.01 M PBS/acetate/borax buffer with different pH values (4, 5, 6, 7, 8, 9, and 10) in the presence of 5 μM BPA at a scan rate of 50 mV/s. (b) Plots of the anodic peak currents of BPA against the pH values (square markers), and plots of the peak potentials of BPA against the pH values (open circle markers). All the experiments were done with an accumulation time of 30 min and 100 rpm magnetic stirring before measurements.

$$\frac{dE_{pa}}{dpH} = 2.303\frac{mRT}{nF} \quad (8)$$

where m is the number of proton, and n is the number of electron. The m/n ratios were calculated to be 1.2 for the BPA oxidation process, which is close to unity. This indicates that the number of protons and electrons involved in the oxidation of BPA were equal, signifying a two-electron-two-proton process.[25]

Voltammetric Determination of BPA. The voltammetric determination of BPA at different concentrations was done by LSV technique.Figure 6(a) shows the LSV curves for the concentrations from 0.05 μM to 30 μM. Figure 6(b) shows the calibration lines for two concentration ranges of 0.05− μM and 5−0 μM. The linear regression equations are as follows:

$$I_p(\mu A) = 10.3C + 0.13(\mu M)(R^2 = 0.9968),\ [0.05 - 5\mu M] \quad (9)$$

$$I_p(\mu A) = 0.85C + 52.3(\mu M)(R^2 = 0.9988),\ [5 - 30\mu M] \quad (10)$$

As shown in Figure 6(b), the GO-MWCNT-βCD/SPE electrode shows high sensitivity for BPA determination in the lower concentration range. However, the sensitivity (slope) of the high concentration linear segment decreases, which could be due to the saturation of the kinetic behavior of the

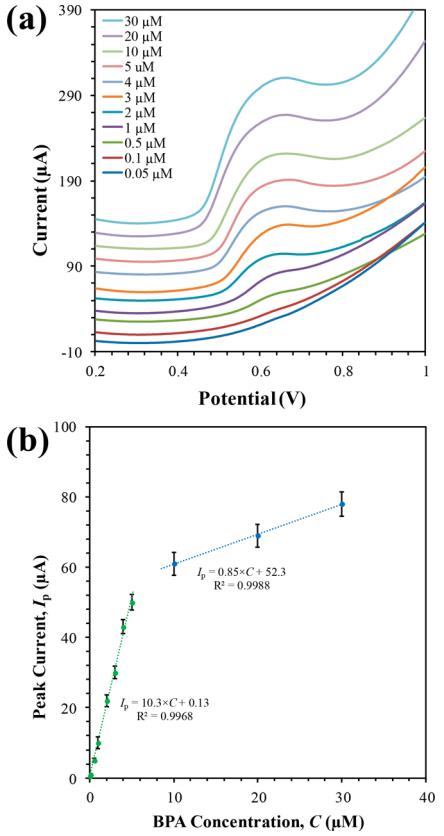

Figure 6. (a) LSVs of GO-MWCNT-βCD/SPE in 0.01 M PBS (pH 7.4) in the presence of 0.005−30 μM BPA. (b) Calibration curve (i.e., peak current vs BPA concentration) for GO-MWCNT-βCD/SPE electrode. All the experiments were done with an accumulation time of 30 min and under 100 rpm magnetic stirring before measurements.

electrode processes during oxidation.[48] We observed that the I_p−C curve started to deviate from its linear behavior and became saturated after 30 μM concentration of BPA. The limit-of-detection (LoD), defined as LoD = 3s/m (where, s is the standard deviation of the blank solution (0.02 μA), and m is the slope of the calibration curve), was estimated to be 6 nM using the first linear segment. The LoD is below the PNEC concentration of BPA in water for aquatic organisms.[10] In Table 1, the linear range and LoD values are compared with other reported literature for the detection of BPA with electrodes based on CNT and graphene. It is observed that the GO-MWCNT-βCD/SPE sensor has achieved very high

Table 1. Comparison of the CNT and Graphene Based Electrochemical Sensors for the Detection of BPA

sensor material	detection method	LoD (nM)	linear range (μM)	reference
CNF/CPE	DPV	50	0.1−60	50
$Li_4Ti_5O_{12}$/MWCNTs/GCE	DPV	78	0.1−10	22
MIP-MWNPE	DPV	22	0.08−100	51
PGA/MWCNT-NH_2/GC	DPV	20	0.1−10	24
SiO_2/rGO−AuNPs/GCE	DPV	5	0.03−10, 10−120	52
GR−IL/GCE	LSV	8	0.02−2	53
GO-MWCNT-βCD/SPE	LSV	6	0.05−5/5−30	this work

https://dx.doi.org/10.1021/acs.analchem.0c00402
Anal. Chem. 2020, 92, 5532−5539

sensitivity and low LoD for the detection of BPA. The enhanced sensing performance of the GO-MWCNT-βCD/SPE sensor can be attributed to the high effective surface area and enhanced host−guest interaction of the sensor. The materials cost for a single GO-MWCNT-βCD/SPE electrode is as low as $0.2 (detailed cost breakdown is shown in Supporting Information Table S1). The cost-effectiveness of the electrode offers feasibility for BPA detection in poor and resource limited areas.

Interference, Stability and Real Water Sample Analysis. The selectivity of the fabricated sensor for the detection of BPA was evaluated in the presence of interfering species. The GO-MWCNT-βCD/SPE electrode showed negligible interference in the presence of common interfering ions such as 5 mM of Na^{2+}, K^{+}, Ca^{2+}, Pb^{2+}, Cl^{-}, SO_4^{2-}, NO_3^{-} ions for the detection of 5 μM BPA. Also, the electrode showed considerable selectivity to 5 μM BPA in the presence of 3 orders of magnitude higher concentrations of other organic species such as 5 mM of ascorbic acid, dopamine, and acetaminophen. The reproducibility and stability of the GO-MWCNT-βCD/SPE electrode were also investigated by preparing five different GO-MWCNT-βCD/SPE electrodes in the same conditions and tested with 5 μM BPA. A relative standard deviation of 2.6% was observed, confirming high reproducibility of the GO-MWCNT-βCD/SPE electrode fabrication. Also, another set of five GO-MWCNT-βCD/SPE electrodes were stored at room temperature for 4 weeks, which showed an RSD of 2.7%. These results indicate that the GO-MWCNT-βCD/SPE has good reproducibility and operating stability for BPA determination.

The practical application of the MWCNT-βCD/GCE sensor was validated by determining the concentration of BPA in real water samples such as tap, bottled, and lake water. The recovery tests of BPA were carried out using LSV through the standard addition method. In this method, the 1 mM BPA stock solutions were added to tap, bottled, and lake water samples to make certain concentrations of BPA (e.g., 0.5 μM, 1 μM, and 2 μM). Table 2 shows that the sensor exhibited an excellent recovery from 96% to 105%. These results indicate that the developed sensor can detect BPA contained in tap, bottled, and lake water samples.

Table 2. Determination Results of BPA in Real Water Samples by LSV

sample	added (μM)	found (μM)[a]	recovery
tap water	0.5	0.48	96%
	1	1.025	102 5%
	2	2.04	102.0%
bottled water	0.5	0.51	102.0%
	1	0.97	97.00%
	2	2.095	104.75
lake water (Ontario Lake)	0.5	0.484	96.80%
	1	0.985	98.50%
	2	2.096	104.8

[a]Average values calculated from three determinations.

CONCLUSIONS

A simple, low-cost and highly sensitive electrochemical sensor for accurate detection of bisphenol A (BPA) based on graphene oxide and β-cyclodextrin functionalized multiwalled carbon nanotubes was fabricated. The sensor demonstrated excellent electrochemical sensing performance toward the detection of BPA with a limit of detection of 6 nM in drinking water, which is below the predicted-no-effect-concentration in water for aquatic organisms. Also, a wide, two-step linear detection ranges from 0.05−5 μM and 5−30 μM was observed. The sensor exhibited high stability, good reproducibility and selectivity for the detection of BPA in the presence of common interfering species such as ascorbic acid, dopamine, and acetaminophen. The sensing performance of the sensor was also investigated using tap, bottled, and lake water spiked with different concentrations of BPA with an excellent recovery of 96% to 105%. The developed sensor shows promises for BPA sensing in water quality monitoring application

ASSOCIATED CONTENT

Supporting Information

The Supporting Information is available free of charge at https://pubs.acs.org/doi/10.1021/acs.analchem.0c00402.

Costs breakdown of the GO-MWCNT-βCD based BPA sensor (PDF)

AUTHOR INFORMATION

Corresponding Author

M. Jamal Deen − *Electrical and Computer Engineering, McMaster University, Hamilton, Ontario L8S 4K1, Canada;* orcid.org/0000-0002-6390-0933; Email: jamal@mcmaster.ca

Author

Arif U. Alam − *Electrical and Computer Engineering, McMaster University, Hamilton, Ontario L8S 4K1, Canada;* orcid.org/0000-0002-5679-0959

Complete contact information is available at: https://pubs.acs.org/10.1021/acs.analchem.0c00402

Author Contributions

The manuscript was written through contributions of all authors who gave approval to the final version of the manuscript.

Notes

The authors declare no competing financial interest.

ACKNOWLEDGMENTS

This research was supported by a Discovery Grant from the Natural Science and Engineering Research Council of Canada, an infrastructure grant from the Canada Foundation for Innovation, a FedDev of Southern Ontario grant, the Canada Research Chair program, and NSERC Green Electronics Network (GreEN, Grant No. 508526-7).

REFERENCES

(1) Liao, C.; Kannan, K. *Environ. Sci. Technol.* **2011**, *45* (21), 9372−9379.

(2) Lim, D. S.; Kwack, S. J.; Kim, K.-B.; Kim, H. S.; Lee, B. M. *J. Toxicol. Environ. Health, Part A* **2009**, *72* (21−22), 1285−1291.

(3) Vandenberg, L. N.; Maffini, M. V.; Sonnenschein, C.; Rubin, B. S.; Soto, A. M. *Endocr. Rev.* **2009**, *30* (1), 75−95.

(4) Karrer, C.; de Boer, W.; Delmaar, C.; Cai, Y.; Crépet, A.; Hungerbühler, K.; von Goetz, N. *Environ. Sci. Technol.* **2019**, *53* (15), 9181−9191.

(5) vom Saal, F. S.; Hughes, C. *Environ. Health Perspect.* **2005**, *113* (8), 926−933.
(6) Alam, A. U.; Qin, Y.; Howlader, M. M. R.; Hu, N.-X.; Deen, M. J. *Sens. Actuators, B* **2018**, *254*, 896−909.
(7) Alam, A. U.; Qin, Y.; Catalano, M.; Wang, L.; Kim, M. J.; Howlader, M. M. R.; Hu, N.-X.; Deen, M. J. *ACS Appl. Mater. Interfaces* **2018**, *10* (25), 21411−21427.
(8) Rubin, B. S. *J. Steroid Biochem. Mol. Biol.* **2011**, *127* (1−2), 27−34.
(9) Wolstenholme, J. T.; Rissman, E. F.; Connelly, J. J. *Horm. Behav.* **2011**, *59* (3), 296−305.
(10) *Bisphenol A (BPA) Action Plan - EPA*; **2010**.
(11) Wetherill, Y. B.; Akingbemi, B. T.; Kanno, J.; McLachlan, J. A.; Nadal, A.; Sonnenschein, C.; Watson, C. S.; Zoeller, R. T.; Belcher, S. M. *Reprod. Toxicol.* **2007**, *24* (2), 178−198.
(12) Peng, Y.; Wang, J.; Wu, C. *J. Agric. Food Chem.* **2019**, *67* (46), 12613−12625.
(13) Richardson, S. D.; Kimura, S. Y. *Anal. Chem.* **2020**, *92* (1), 473−505.
(14) Hersey, M.; Berger, S. N.; Holmes, J.; West, A.; Hashemi, P. *Anal. Chem.* **2019**, *91* (1), 27−43.
(15) Hu, L.; Fong, C.-C.; Zhang, X.; Chan, L. L.; Lam, P. K. S.; Chu, P. K.; Wong, K.-Y.; Yang, M. *Environ. Sci. Technol.* **2016**, *50* (8), 4430−4438.
(16) Apodaca, D. C.; Pernites, R. B.; Ponnapati, R.; Del Mundo, F. R.; Advincula, R. C. *Macromolecules* **2011**, *44* (17), 6669−6682.
(17) Ho, T. D.; Zhang, C.; Hantao, L. W.; Anderson, J. L. *Anal. Chem.* **2014**, *86* (1), 262−285.
(18) Huang, N.; Liu, M.; Li, H.; Zhang, Y.; Yao, S. *Anal. Chim. Acta* **2015**, *853* (1), 249−257.
(19) Hou, K.; Huang, L.; Qi, Y.; Huang, C.; Pan, H.; Du, M. *Mater. Sci. Eng., C* **2015**, *49*, 640−647.
(20) Wang, Y.-C.; Cokeliler, D.; Gunasekaran, S. *Electroanalysis* **2015**, *27* (11), 2527−2536, DOI: 10.1002/elan.201500120.
(21) Wan, J.; Si, Y.; Li, C.; Zhang, K. *Anal. Methods* **2016**, *8*, 3333−3338.
(22) Wang, W.; Yang, X.; Gu, Y.; Ding, C.; Wan, J. *Ionics* **2015**, *21* (3), 885−893.
(23) Alam, A. U.; Qin, Y.; Nambiar, S.; Yeow, J. T. W.; Howlader, M. M. R.; Hu, N.-X.; Deen, M. J. *Prog. Mater. Sci.* **2018**, *96*, 174−216.
(24) Lin, Y.; Liu, K.; Liu, C.; Yin, L.; Kang, Q.; Li, L.; Li, B. *Electrochim. Acta* **2014**, *133*, 492−500.
(25) Yin, H.; Zhou, Y.; Xu, J.; Ai, S.; Cui, L.; Zhu, L. *Anal. Chim. Acta* **2010**, *659* (1−2), 144−150.
(26) Kazane, I.; Gorgy, K.; Gondran, C.; Spinelli, N.; Zazoua, A.; Defrancq, E.; Cosnier, S. *Anal. Chem.* **2016**, *88* (14), 7268−7273.
(27) Pei, D.-N.; Zhang, A.-Y.; Pan, X.-Q.; Si, Y.; Yu, H.-Q. *Anal. Chem.* **2018**, *90* (5), 3165−3173.
(28) Dassios, K. G.; Alafogianni, P.; Antiohos, S. K.; Leptokaridis, C.; Barkoula, N.-M.; Matikas, T. E. *J. Phys. Chem. C* **2015**, *119* (13), 7506−7516.
(29) Tiwari, J. N.; Vij, V.; Kemp, K. C.; Kim, K. S. *ACS Nano* **2016**, *10* (1), 46−80.
(30) Crini, G.; Morcellet, M. *J. Sep. Sci.* **2002**, *25* (13), 789−813.
(31) Morin-Crini, N.; Crini, G. *Prog. Polym. Sci.* **2013**, *38* (2), 344−368.
(32) Menuel, S.; Joly, J.-P.; Courcot, B.; Elysée, J.; Ghermani, N.-E.; Marsura, A. *Tetrahedron* **2007**, *63* (7), 1706−1714.
(33) Thatiparti, T. R.; Shoffstall, A. J.; von Recum, H. A. *Biomaterials* **2010**, *31* (8), 2335−2347.
(34) Alsbaiee, A.; Smith, B. J.; Xiao, L.; Ling, Y.; Helbling, D. E.; Dichtel, W. R. *Nature* **2016**, *529* (7585), 190−194.
(35) Liu, J.; Yang, Y.; Bai, J.; Wen, H.; Chen, F.; Wang, B. *Anal. Chem.* **2018**, *90* (5), 3621−3627.
(36) Yu, X.; Chen, Y.; Chang, L.; Zhou, L.; Tang, F.; Wu, X. *Sens. Actuators, B* **2013**, *186*, 648−656.
(37) Gao, Y.; Cao, Y.; Yang, D.; Luo, X.; Tang, Y.; Li, H. *J. Hazard. Mater.* **2012**, *199−200*, 111−118.
(38) Li, Y.; Gao, Y.; Cao, Y.; Li, H. *Sens. Actuators, B* **2012**, *171−172*, 726−733.
(39) Abbaspour, A.; Noori, A. *Biosens. Bioelectron.* **2011**, *26* (12), 4674−4680.
(40) Alsbaiee, A.; Smith, B. J.; Xiao, L.; Ling, Y.; Helbling, D. E.; Dichtel, W. R. *Nature* **2016**, *529* (7585), 190−194.
(41) Habibi, B.; Jahanbakhshi, M.; Pournaghi-Azar, M. H. *Anal. Biochem.* **2011**, *411* (2), 167−175.
(42) Ramnani, P.; Saucedo, N. M.; Mulchandani, A. *Chemosphere* **2016**, *143*, 85−98.
(43) Baptista, F. R.; Belhout, S. a.; Giordani, S.; Quinn, S. J. *Chem. Soc. Rev.* **2015**, *44*, 4433−4453.
(44) Bard, A. J.; Faulkner, L. R. *Electrochemical Methods*, 2nd ed.; Wiley: New York, 2011.
(45) Yaman, Y.; Abaci, S. *Sensors* **2016**, *16* (6), 756.
(46) Nicholson, R. S.; Shain, I. *Anal. Chem.* **1964**, *36* (4), 706−723.
(47) Brownson, D. A. C.; Banks, C. E. Interpreting Electrochemistry. In *The Handbook of Graphene Electrochemistry*; Springer London: London, 2014; pp 23−77. DOI: 10.1007/978-1-4471-6428-9_2.
(48) Wang, J. Y.; Su, Y. L.; Wu, B. H.; Cheng, S. H. *Talanta* **2016**, *147*, 103−110.
(49) Laviron, E. *J. Electroanal. Chem. Interfacial Electrochem.* **1974**, *52* (3), 355−393.
(50) Sun, J.; Liu, Y.; Lv, S.; Huang, Z.; Cui, L.; Wu, T. *Electroanalysis* **2016**, *28*, 439−444.
(51) Chen, Z.; Tang, C.; Zeng, Y.; Liu, H.; Yin, Z.; Li, L. *Anal. Lett.* **2014**, *47* (6), 996−1014.
(52) Liu, E.; Zhang, X. *Anal. Methods* **2014**, *6*, 8604−8612.
(53) Jing, P.; Zhang, X.; Wu, Z.; Bao, L.; Xu, Y.; Liang, C.; Cao, W. *Talanta* **2015**, *141*, 41−46.

https://dx.doi.org/10.1021/acs.analchem.0c00402
Anal. Chem. 2020, 92, 5532−5539